



Effect of angstrom-scale surface roughness on the self-assembly of polystyrene-polydimethylsiloxane block copolymer

Shreya Kundu^{1,2}, Ramakrishnan Ganesan^{2,3}, Nikita Gaur¹, Mohammad S. M. Saifullah², Hazrat Hussain⁴, Hyunsoo Yang¹ & Charanjit S. Bhatia¹

¹Department of Electrical and Computer Engineering, National University of Singapore, 21 Lower Kent Ridge Road, Singapore 117576, Republic of Singapore, ²Institute of Materials Research and Engineering, A* STAR (Agency for Science, Technology and Research), 3 Research Link, Singapore 117602, Republic of Singapore, ³Department of Chemistry, Birla Institute of Technology & Science, Pilani – Hyderabad Campus, Jawahar Nagar, Shameerpet Mandal, Hyderabad – 500 078 (Andhra Pradesh), India, ⁴Department of Chemistry, University College of Sciences (Shankar), Abdul Wali Khan University, Mardan 23200 (Khyber Pakhtunkhwa), Pakistan.

Received
30 January 2012

Accepted
14 August 2012

Published
31 August 2012

Correspondence and requests for materials should be addressed to M.S.M.S. (saifullahm@imre.a-star.edu.sg)

Self-assembly of block copolymers has been identified as a potential candidate for high density fabrication of nanostructures. However, the factors affecting its reliability and reproducibility as a patterning technique on various kinds of surfaces are not well-established. Studies pertaining to block copolymer self-assembly have been confined to ultra-flat substrates without taking into consideration the effect of surface roughness. Here, we show that a slight change in the angstrom-scale roughness arising from the surface of a material creates a profound effect on the self-assembly of polystyrene-polydimethylsiloxane block copolymer. Its self-assembly was found to be dependent on both the root mean square roughness (R_{rms}) of the surface and the type of solvent annealing system used. It was observed that surface with $R_{\text{rms}} < 5.0 \text{ \AA}$ showed self-assembly. Above this value, the kinetic hindrance posed by the surface roughness on the block copolymer leads to its conforming to the surface without observable phase separation.

Syntheses of arrays of closely spaced nanostructures with different morphologies have been made possible by the self-assembly of di- and tri-block copolymers. The morphology of these self-assembled domains can be spherical, lamellar or cylindrical based on the volume fraction of the blocks and is attainable on sub-20 nm scale^{1–11}. The versatility of this self-assembly technique has drawn the attention of the high density data storage industry to use it as a scalable, high-throughput and low cost nanofabrication method to fabricate bit patterned media (BPM)^{12–14}. However, the flexibility provided by self-assembly goes beyond the attainment of features on sub-20 nm scale. The dimension, geometry and interspacing of the blocks are controlled by their molecular weight and by employing a blend of block copolymer and homopolymer¹⁵. Thermal annealing of the block copolymers^{16,17} as well as application of localized electric¹⁸ and large amplitude oscillatory shear fields¹⁹ to the spin-coated films have been shown to dictate the alignment of blocks. An alternative and rapid route involving solvent vapor annealing of block copolymer films has also proven to be effective in regulating the orientation and morphology of the microdomains^{20–25}. Long range ordering and strict position control of these features has also been realized through the use of chemically pre-patterned templates¹, graphoepitaxy^{2–3}, topographical patterns⁴ or by introducing nanoscopic facets on the surface⁵. These diverse features of self-assembly make it an ideal contender for accomplishing the goal of high density patterning of nanostructures. In spite of these advantages, it is not clear as to what factors adversely affect the reliability and reproducibility of self-assembly on different substrate surfaces. It should be noted that almost all the self-assembly studies so far reported are on ‘idealized’ surfaces such as highly polished silicon or single crystal substrates^{1–13,15,16}. There has hardly been any emphasis on the effect of surface roughness of the substrate on the self-assembly of block copolymers.

Magnetic thin films are produced by magnetron sputtering and they exhibit nanoscopic surface roughness^{26,27}. Depending on the sputtering conditions such as incident power, pressure, temperature and seed-layer, the degree of surface roughness can be varied on an angstrom-scale, giving rise to either continuous or granular magnetic

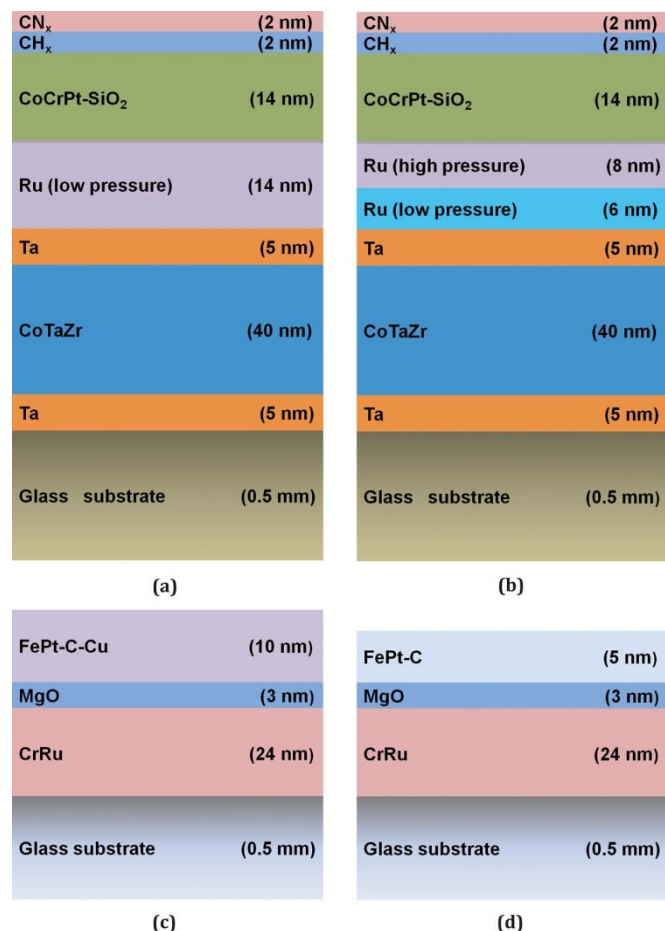


Figure 1 | Schematic representation of different layers of (a) continuous CoCrPt-SiO₂, (b) granular CoCrPt-SiO₂, (c) granular FePt-C-Cu and (d) granular FePt-C magnetic media.

media. Therefore, magnetic media serves as an ideal system for a systematic study of the self-assembly of block copolymers on surfaces with varying roughnesses. In this work, the effect of angstrom-scale surface roughness on the self-assembly of polystyrene-polydimethylsiloxane (PS-*b*-PDMS) block copolymer using solvent annealing is reported. In addition, the efficacy of self-assembly employing two solvent annealing systems as a function of surface roughness is also studied.

Results

Substrates with varying angstrom-scale roughness. Continuous and granular CoCrPt-SiO₂, granular FePt-C-Cu and FePt-C magnetic media were prepared by magnetron sputtering. All the layers of CoCrPt-SiO₂ media were deposited at room temperature. To improve the adhesion of the deposited layers to the glass substrate, a tantalum (Ta) layer was grown on it. Cobalt-tantalum-zirconium (CoTaZr) alloy was employed as the soft magnetic underlayer essential for perpendicular magnetic recording. A second Ta layer was used as the seed-layer to provide a clean and smooth surface to the underlayer. In the case of continuous media, a single ruthenium (Ru) interlayer was deposited at low argon pressure (3 mTorr) to promote a good crystallographic texture of the CoCrPt-SiO₂ magnetic layer (6 mTorr) [Figure 1(a)]. On the other hand, the granular media comprised of two Ru interlayers. The first Ru layer improved the texture, whereas the second Ru layer, grown at a higher argon pressure (60 mTorr), caused grain segregation in the top recording layer (deposited at a pressure of 60 mTorr), leading to a higher surface roughness [Figure 1(b)]²⁸. On both continuous and granular CoCrPt-SiO₂ media, carbon was deposited in hydrogen and

nitrogen environment to form a carbon overcoat on top of the media samples.

Granular FePt-C-Cu and FePt-C samples were grown as follows: Chromium-ruthenium (CrRu) alloy deposited at 400 °C gave rise to a (002) texture which in turn induced the (001) texture in the FePt alloy through heteroepitaxy. A magnesium oxide (MgO) layer grown at 400 °C was introduced as a buffer layer between CrRu and FePt-C-Cu/FePt-C to avoid the diffusion of Cr into the recording layer. Moreover, it also promoted a good crystallographic texture of the recording layer. Both CrRu and MgO were deposited at low argon pressure (1.5 mTorr) to provide a smoother surface to the FePt-C-Cu and FePt-C layers to grow [Figure 1(c) and 1(d)]. The MgO layer was RF etched at 50 W for 5 minutes to planarize it further prior to the deposition of FePt-C-Cu and FePt-C layers. FePt-C-Cu was deposited at 400 °C and 5 mTorr argon pressure. However, the desired *L1*₀ ordered phase was not attained (see Supplementary Information). On the other hand, FePt-C was deposited at 600 °C and 3 mTorr argon pressure to obtain the *L1*₀ phase. Deposition at elevated temperature was accompanied by grain growth, thereby resulting in higher roughness²⁹.

For the self-assembly of PS-*b*-PDMS on magnetic media with different surface roughnesses, chemical functionalization of the substrate is essential. Hydroxyl-terminated PS and PDMS brushes serve this purpose by bonding with the native oxide layer on top of the silicon substrates²⁹. On surfaces other than silicon, we found TranSpin™ (a proprietary material sold by Molecular Imprints, Inc.) to be an alternative choice. TranSpin is used as an adhesion promoter and for planarizing silicon wafers in step-and-flash nanoimprint lithography³⁰. TranSpin has a water contact angle of 83° which is very close to that of PS (~90°)³¹ than of PDMS (110°)³². From the wetting properties, it can be inferred that PS and TranSpin have similar surface energies. Therefore, TranSpin will have more interfacial interaction with PS than with PDMS. This causes PS, the major block, to form a matrix. In contrast, the PDMS block organizes into spherical dots. When TranSpin was spin-coated at 3000 rpm and baked at 195 °C for 90 seconds, an organic layer of < 2 nm thickness was obtained. Ellipsometry measurement indicated the thickness of the planarizing layer to be ~1.7 nm. During solvent annealing, this thin organic layer enhances the chain mobility of the blocks by providing them with a softer platform. TranSpin also modifies the surface roughness of magnetic media to a small extent and enables the study of self-assembly of PS-*b*-PDMS on a wider range of surfaces. More importantly, TranSpin eliminates any effect on self-assembly, apart from the surface roughness arising from the magnetic media underneath.

The topographies of the continuous and granular media samples were studied using SEM and AFM. Figure 2 and Table I show root mean square roughnesses (i.e., *R*_{rms}) of different magnetic media exhibiting angstrom-scale variation. Another roughness parameter which can be considered is the peak-to-peak mean roughness depth (*R*_t). *R*_t provides information regarding the coating quality of a material. From both *R*_{rms} and *R*_t values, it can be inferred that a more plateau surface is achieved after coating the media structures with TranSpin.

Effect of roughness on the self-assembly of PS-*b*-PDMS. The self-assembly of PS-*b*-PDMS was carried out on as-deposited samples as well as on samples coated with a layer of TranSpin. The results are shown in Figure 3. High resolution insets shown in Figure 3 were used to compute their corresponding Fast Fourier Transform (FFT) images (Figure 4). On continuous CoCrPt-SiO₂ media without any TranSpin underlayer (*R*_{rms} = 3.3 Å), the dots did not appear to be well separated when solvent annealed in tetrahydrofuran (THF). This is because THF preferentially swelled PS more than PDMS, and therefore, the PDMS block did not have enough mobility to form dots. However, when the 6:1 toluene-heptane solvent mixture was

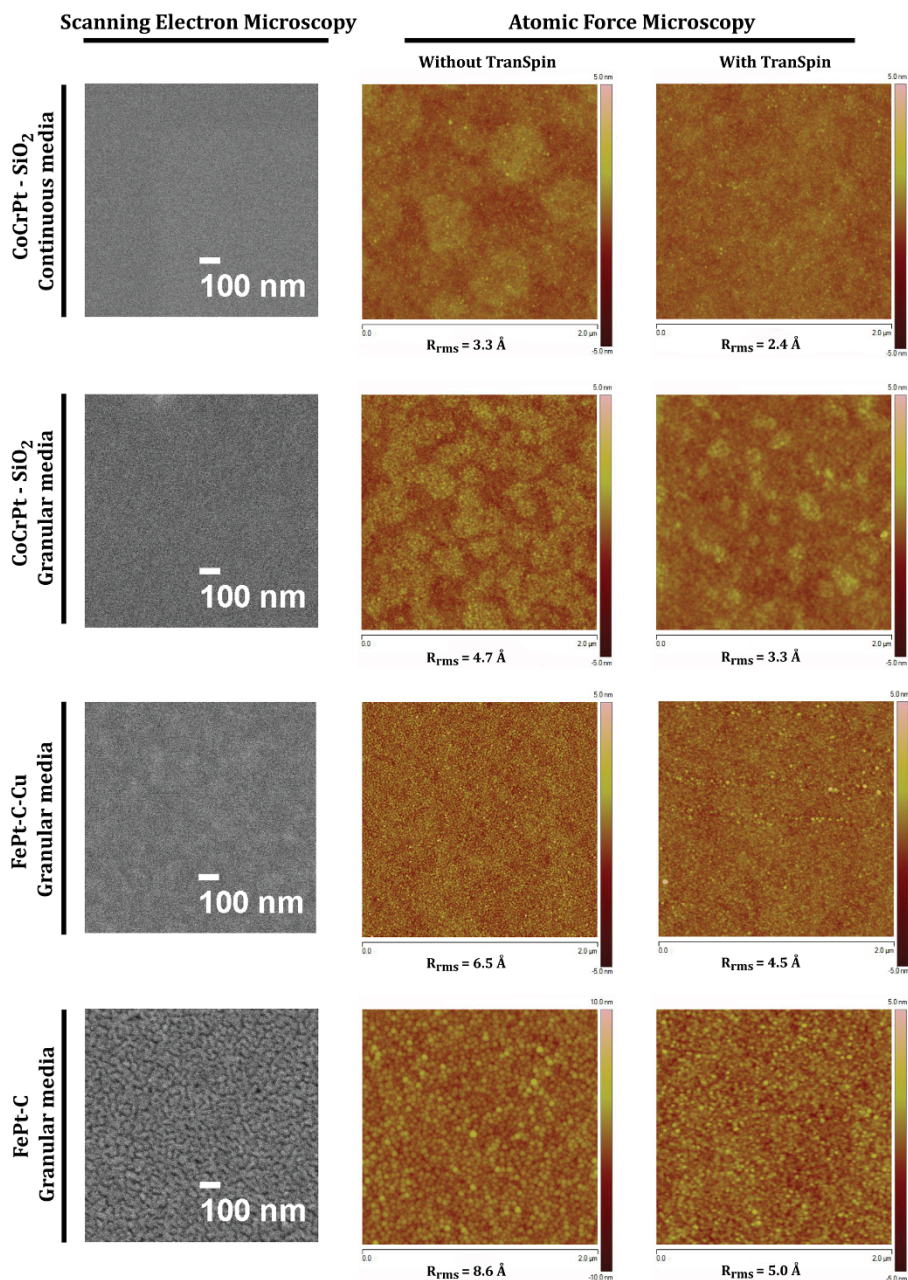


Figure 2 | SEM and AFM images of the magnetic media with and without the TranSpin layer. The surface roughness of granular FePt-C magnetic media is reduced to 8.2 Å (R_{rms}) when coated with a layer of TranSpin. The R_{rms} was further reduced to 5.0 Å when five layers of TranSpin were spin-coated on the granular FePt-C media.

Table 1 | Root mean square (RMS) roughness (R_{rms}) and peak-to-peak mean roughness depth (R_i) of magnetic media calculated using AFM scans. The values of R_{rms} and R_i represent mean and standard deviation from eight scans (scan area = $2 \mu\text{m} \times 2 \mu\text{m}$) at different locations on the sample. Unless stated, only one layer of TranSpin was coated

Magnetic media type/ Roughness parameters	Continuous CoCrPt-SiO ₂		Granular CoCrPt-SiO ₂		Granular FePt-C-Cu		Granular FePt-C		
	Without TranSpin	With TranSpin	Without TranSpin	With TranSpin	Without TranSpin	With TranSpin	Without TranSpin	With TranSpin	With TranSpin (5 layers)
R_{rms} : Root mean square roughness (Å)	3.3±0.1	2.4±0.2	4.7±0.2	3.3±0.1	6.5±0.3	4.5±0.1	8.6±0.1	8.2±0.1	5.0±0.2
R_i : peak-to-peak roughness (Å)	9.9±0.3	7.2±0.3	13.0±0.6	9.2±0.5	22.2±0.7	14.2±0.1	26.0±0.2	25.0±0.4	15.0±0.1

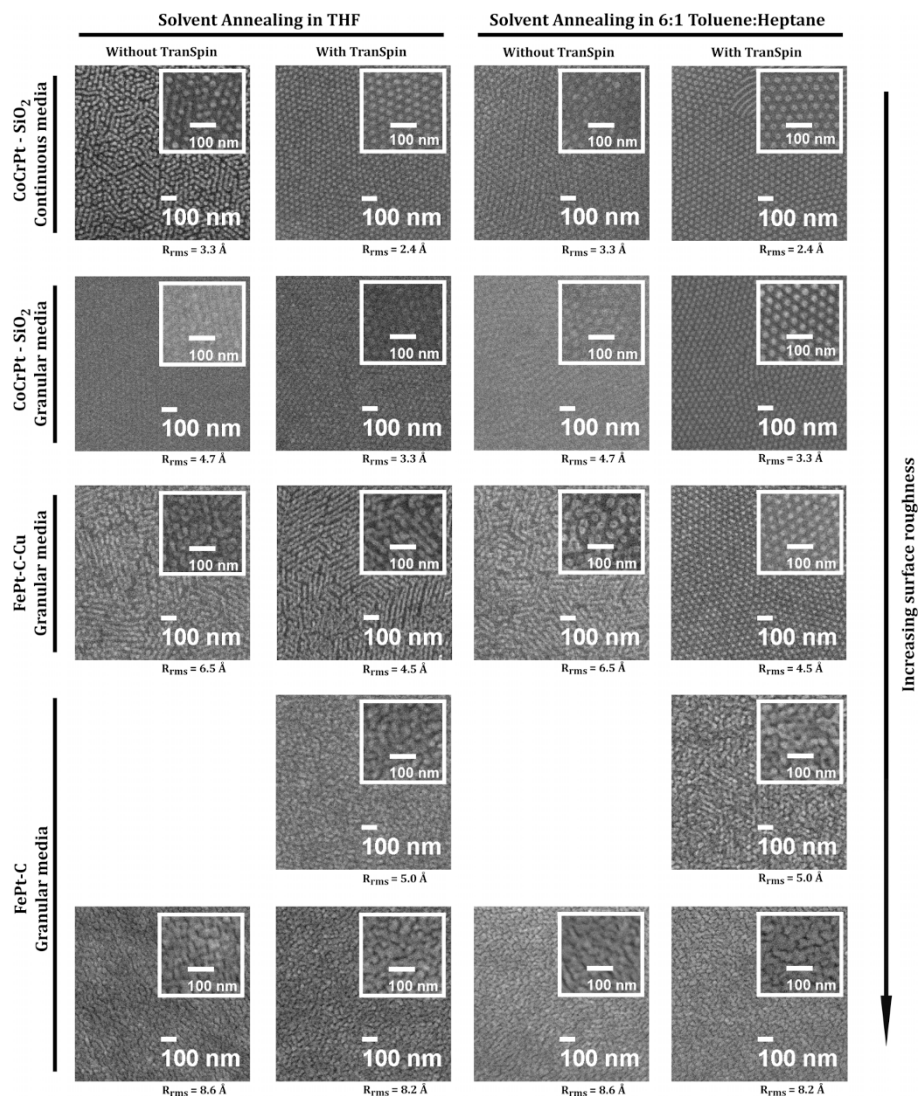


Figure 3 | SEM images of the self-assembly of PS-*b*-PDMS on magnetic media with varying surface roughnesses and solvent annealed in THF and 6:1 toluene-heptane solvent systems. The surface roughness of granular FePt-C magnetic media was modified by spin-coating one and five layers of TranSpin to achieve R_{rms} of 8.2 Å and 5.0 Å, respectively.

employed for annealing, the self-assembly showed marginal improvement with some PDMS dot patterns exhibiting partial isolation from one another. On the other hand, spherical dots were clearly visible when self-assembly of PS-*b*-PDMS was carried out on the TranSpin-coated continuous media samples ($R_{rms}=2.4 \text{ \AA}$) and solvent annealed in THF and the 6:1 toluene-heptane mixture. Apart from reducing the surface roughness, the TranSpin layer also increased chain mobility of the blocks, thereby enabling self-assembly. This is also evident as the first- and higher-order peaks in the corresponding FFT images became sharper (Figure 4). Not surprisingly, a similar trend was also observed when self-assembly of PS-*b*-PDMS was carried out on the Si wafer surface ($R_{rms}=1.5 \text{ \AA}$) which is smoother than continuous CoCrPt-SiO₂ media samples (see Supplementary Information).

On a slightly rougher granular CoCrPt-SiO₂ magnetic media ($R_{rms}=4.7 \text{ \AA}$), without the TranSpin underlayer, solvent annealing in THF barely showed the appearance of dots. However, on the TranSpin-coated samples ($R_{rms}=3.3 \text{ \AA}$), a marginal improvement in the self-assembly in THF vapor was observed, perhaps due to increased chain mobility. The existence of partial self-assembly was confirmed by the presence of first-order spots in the FFT image (Figure 4). Comparing the block copolymer self-assembly using THF

vapor on the TranSpin-coated continuous and granular CoCrPt-SiO₂ magnetic media, it was seen that the latter's slightly higher roughness hindered phase separation of the individual blocks. When the 6:1 toluene-heptane mixture was used for solvent annealing, an excellent self-assembly was observed on the granular magnetic media (Figure 3). Unsurprisingly, the FFT of the self-assembled dots showed sharp first- and higher-order spots. However, a slightly diffused halo around the first-order spots was observed in the case of TranSpin-coated granular CoCrPt-SiO₂ media, suggesting a minor degradation in self-assembly. The preferential swelling of PS by toluene and PDMS by heptane enabled the blocks to override the roughness barrier and consequently phase separate distinctly. In the TranSpin-coated continuous and granular media, cylinders along with the dots were observed when solvent annealed in the 6:1 toluene-heptane mixture. Heptane uptake by the PDMS block on continuous media increases its effective volume fraction, thus tending to change its morphology from spherical to lamellar, as suggested by the phase diagram²³.

The surface roughness rose to $R_{rms}=6.5 \text{ \AA}$ when the magnetic media was changed to FePt-C-Cu. Self-assembly was *only seen* on the TranSpin-coated FePt-C-Cu substrate ($R_{rms}=4.5 \text{ \AA}$) when the block copolymer was solvent annealed in the 6:1 toluene-heptane

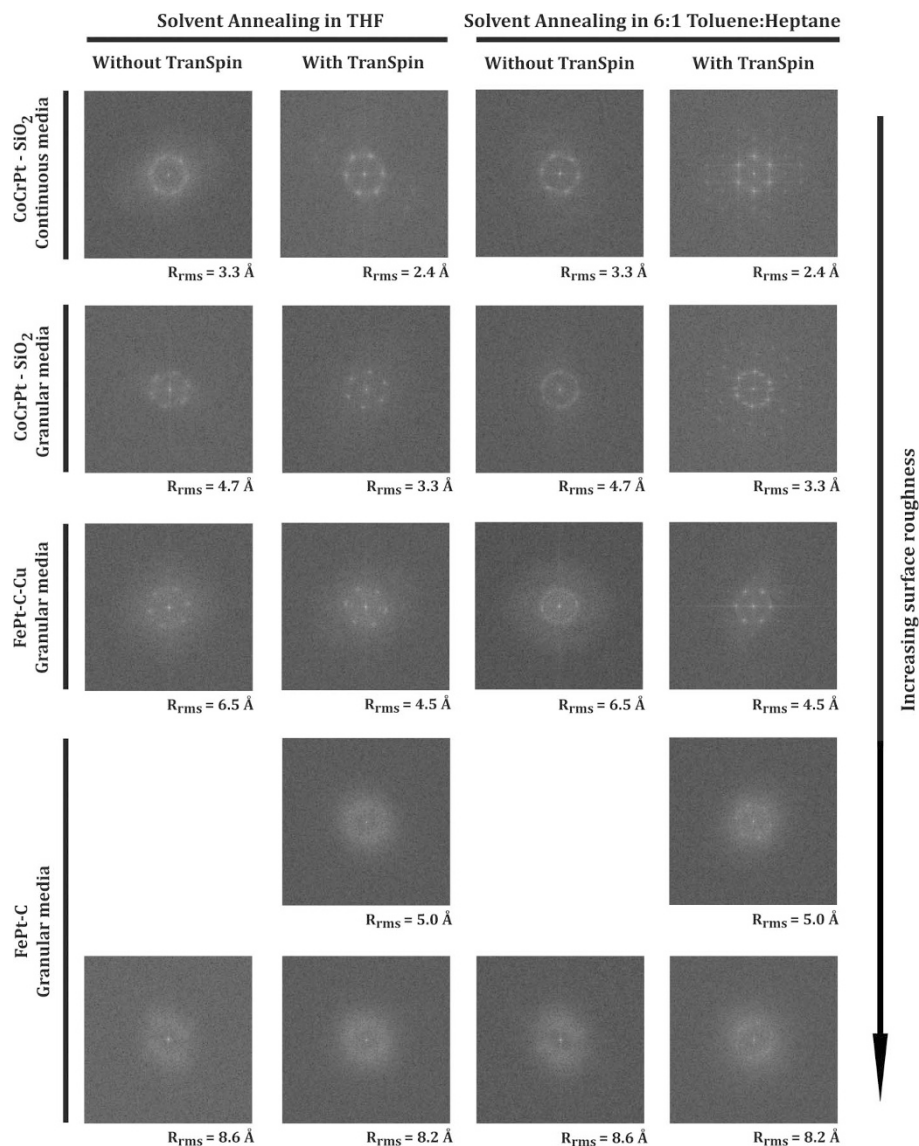


Figure 4 | Fast-Fourier transform images of self-assembly of PS-*b*-PDMS on magnetic media with varying surface roughnesses and solvent annealed in THF and 6 : 1 toluene-heptane solvent systems. These images were computed from their corresponding high resolution insets shown in Figure 3.

mixture. However, the dots did not appear perfectly spherical as had been observed previously on the TranSpin-coated continuous and granular CoCrPt-SiO₂ media surfaces. Therefore, this can be viewed as a gradual deterioration of the self-assembly of PS-*b*-PDMS with increasing surface roughness (Figure 3). This is reinforced by the fact that, unlike continuous and granular CoCrPt-SiO₂ media surfaces, the FFT image of self-assembly on TranSpin-coated granular FePt-C-Cu showed first-order and extremely weak higher order spots. Solvent annealing of PS-*b*-PDMS on as-deposited and TranSpin-coated FePt-C-Cu employing THF vapor resulted in the formation of randomly oriented connected dots. Similar observation was also made when the block copolymer, spin-coated on the as-deposited sample, was annealed in the 6 : 1 toluene-heptane vapor. However, a few isolated dots were seen amongst the connected dots. This is most likely due to heptane providing the PDMS block a slight increase in chain mobility to attempt to form dots.

The SEM images of self-assembly of PS-*b*-PDMS on as-deposited continuous CoCrPt-SiO₂ and granular FePt-C-Cu media samples showed the appearance of randomly connected dots when annealed in the THF vapor. The dots on continuous CoCrPt-SiO₂ media were

on the verge of separating from one another. However, the PDMS block could not segregate completely into dots due to lack of the required chain mobility which has been shown to be provided by the use of the TranSpin layer. On the other hand, the dots on the FePt-C-Cu media tend to aggregate rather than moving apart due to the higher surface roughness. Spinning a layer of TranSpin on the sample surface did not reduce the surface roughness significantly. Hence, the dots remained randomly connected. Similar observation was made for self-assembly on the *bare* samples employing 6 : 1 toluene-heptane mixture. As R_{rms} was increased from 3.3 Å to 4.7 Å, the dots appeared fainter. However, when R_{rms} rose to 6.5 Å, randomly connected dots came into existence. It may be conjectured that the energy required by the PDMS block to surmount the energy barrier posed by the increased surface roughness was higher than the energy cost involved in remaining in an agglomerated form. This is supported by the FFT images of the self-assembly which show the presence of weak first-order spots, suggesting the absence of ordered dots (Figure 4).

The FePt-C film is the roughest among the four magnetic media prepared for this study (Figure 2). The roughness arising from bare



FePt-C media ($R_{\text{rms}}=8.6 \text{ \AA}$) was modified by applying one ($R_{\text{rms}}=8.2 \text{ \AA}$) and five layers of TranSpin ($R_{\text{rms}}=5.0 \text{ \AA}$). At $R_{\text{rms}}=5.0 \text{ \AA}$, there was no indication of self-assembly of PS-*b*-PDMS on FePt-C samples when annealed in the THF solvent vapor. In the case of 6 : 1 toluene-heptane solvent system, the phase separation of the blocks appeared to be restricted by the high surface roughness of the media, resulting in an appearance of randomly connected dots. However, when the amount of heptane was increased twofold in the solvent mixture spherical dots were seen with a weak footing on the magnetic grains and they sparsely populated the sample (see Supplementary Information). On surfaces with $R_{\text{rms}} > 5.0 \text{ \AA}$, no self-assembly was observed and their topography appeared similar to that of bare FePt-C surface (Figure 3). The FFT image showed a diffused halo (Figure 4). This observation can be attributed to the immobility of PS-*b*-PDMS block copolymer, leading to its conformation onto such rough surfaces. The presence of the TranSpin layer seems to be ineffective to enable the block copolymer to overcome the barrier posed by the surface roughness.

Discussion

The self-assembly of PS-*b*-PDMS is kinetically hindered by surface roughness. Solvent annealing of the blocks is an effective way to swell them, improve their chain mobility and thus alleviate the impediment posed by surface roughness. When THF was employed for solvent annealing on the TranSpin-coated continuous CoCrPt-SiO₂ media, it preferentially swelled up the PS block. The PDMS block, in contrast, to avoid unfavourable interaction with THF, aggregated into spherical dots. On the granular CoCrPt-SiO₂ media coated with TranSpin, the PDMS block lacked sufficient mobility to overcome the roughness-induced blockade and organize into dots. However, on switching the solvent annealing system from THF to the 6 : 1 toluene-heptane mixture, the PDMS block became mobile enough to self-assemble into dot patterns. PDMS is soluble in heptane and by deriving the required energy from interaction with the latter, it was able to surmount the kinetic hindrance.

Faintly visible dots, as seen on the TranSpin-coated granular CoCrPt-SiO₂ media, disappeared on a slightly rougher FePt-C-Cu surface when the block copolymer was annealed in the THF vapor, and were replaced by the randomly connected dots. On the other hand, using the 6 : 1 toluene-heptane mixture for solvent annealing provided the blocks with sufficient amount of energy to override the slight increase in roughness and self-assemble into dot-like features, albeit not perfectly spherical.

However, when R_{rms} reached close to 5.0 \AA , mobility of both the blocks was reduced even further, thus destroying self-assembly. Increasing the amount of heptane in toluene-heptane mixture did not appear to improve the self-assembly on such rough surfaces. Therefore, the effectiveness of a solvent system to induce self-assembly of PS-*b*-PDMS is limited by surface roughness. The FFT images of self-assembly also show a trend indicating the degradation of self-assembly with increasing surface roughness. The surface with least roughness shows sharp first- and higher-order spots. However, with increasing surface roughness, a diffused halo appears around the first-order spots and the higher-order spots disappear. When the $R_{\text{rms}} > 5.0 \text{ \AA}$, only the diffused halo remains.

In a block copolymer, the chains are usually in the form of a collapsed globule. It has been suggested that solvent diffusion through the film creates a concentration gradient perpendicular to the film surface which enables the transition of the block copolymer film from a disordered to an ordered state from the substrate to the air surface^{20,21}. In our case, the block copolymer film closest to the bottom has to move over the surface roughness barrier first and undergo a transition to the ordered state. This transition is then propagated upwards throughout the entire film. However, if the surface roughness becomes insurmountable for the block copolymer film closest to the substrate surface during solvent annealing, the

ordering is no longer observed. This results in the block copolymer conforming to the surface of magnetic media.

Block copolymers self-assemble in various morphologies on a substrate. Our study has shown that the surface roughness of a substrate plays an important role in governing the self-assembly. Just like the changes observed in spherical morphology of PS-*b*-PDMS with increasing roughness of the substrate, the lamellar morphology is also affected. However, the lamellar structures face a consequence which is different to the spherical morphology when surface roughness of the substrate is increased (see Supplementary Information).

Self-assembly is a process which exhibits a balance of the intermolecular forces between the homopolymer units and the chemical interaction of these units with the solvent system used for annealing. Qualitatively, the Gibbs free energy model is often used to describe the thermodynamics of self-assembly^{25,33}

$$\Delta G_{SA} = \Delta H_{SA} - T\Delta S_{SA}$$

where ΔH_{SA} is the enthalpy change taking place due to the intermolecular forces between the covalently bonded assembling units as well as their interaction with the solvent vapor causing the phase separation of the blocks. ΔS_{SA} is the entropy change taking place in the system as the polymer units arrange from a disordered to an ordered state and is negative. Hence, to achieve self-assembly on a surface, the Gibbs free energy change, ΔG_{SA} , must be negative as the system goes from a disorder-to-order transition. Therefore, ΔH_{SA} should be negative and in excess of the other counter-balancing term in the equation, i.e., $T\Delta S_{SA}$ ³³. This free energy model for self-assembly assumes a *smooth ideal surface* and only involves the intermolecular interactions between the two blocks in a copolymer and solvent vapor.

However, when the self-assembly process with the same block copolymer and solvent system is carried out on surfaces with finite roughness values, the free energy model with above parameters cannot explain the experimental observation of the gradual degradation of self-assembled structures with increasing roughness of the substrates. Therefore, we introduce a term ΔE_R which represents the additional energy required by the polymer chains to diffuse over the corrugated surface. Taking into account the energy barrier posed by surface roughness, the modified Gibbs free energy model can be expressed as

$$\Delta G_{SA*} = \Delta H_{SA*} - T\Delta S_{SA*}$$

where $\Delta H_{SA*} = \Delta H_{SA} + \Delta E_R$.

For self-assembly to be a spontaneous process on a substrate surface exhibiting roughness

$$\Delta H_{SA*} > |-T\Delta S_{SA*}|$$

$$\text{or } \Delta H_{SA} + \Delta E_R > |-T\Delta S_{SA*}|$$

In other words, ΔG_{SA*} must be negative, suggesting that ΔH_{SA*} is negative and exceeds the absolute value the entropy term $T\Delta S_{SA*}$. However, when the surface roughness exceeds certain critical value then ΔG_{SA*} becomes positive, leading to the ceasing of self-assembly and the block copolymer conforming to the substrate surface.

In conclusion, the self-assembly of PS-*b*-PDMS using solvent annealing was studied on substrate surfaces with R_{rms} ranging from 2.4 \AA to 8.6 \AA . The smoothest surface was achieved by coating the continuous CoCrPt-SiO₂ media with a layer of TranSpin. Phase separation was easily observed on these substrates when THF and 6 : 1 toluene-heptane solvent annealing systems were used. In contrast, self-assembly on the bare continuous CoCrPt-SiO₂ media displaying a slightly higher roughness resulted in poorly ordered dots. This suggests the necessity to use TranSpin to provide the polymer chains with a softer platform for improved chain mobility leading to the phase separation. When the surface roughness of the



TranSpin-coated substrate was increased to 3.3 Å, well-segregated dots could no longer be observed on the surface when annealed using THF. Here the solvent was not able to provide the minor PDMS block sufficient energy to move over the rougher surface which kinetically hindered the formation of the dots. On the other hand, the 6 : 1 toluene-heptane solvent annealing system succeeded in providing self-assembly on the TranSpin coated-surfaces with roughness > 2.4 Å, but a slight deterioration in the shape of the dots was observed as roughness was increased to 4.5 Å. For roughnesses above 5.0 Å, the 6 : 1 toluene-heptane solvent annealing system was ineffective in obtaining the desired spherical morphology. Therefore, the ability of a solvent system to swell individual blocks to overcome the surface roughness barrier reaches a limit when the roughness exceeds certain critical value. At this point self-assembly fails and the block copolymer conforms to the substrate surface.

Nanofabrication by conventional techniques such as optical, electron and nanoimprint lithographies show good reliability and reproducibility³⁴. The former two, due to the availability of good depth of focus and ability to pattern thick resists, are quite immune to the presence of surface roughness. On the other hand, nanoimprint lithography, especially using soft molds, can be used to imprint rough and uneven surfaces. Self-assembly, unlike conventional lithography methods, enables the creation of nanopatterns through physical movement of the polymer chains in a block copolymer. Our work has clearly shown that such a movement is sensitive to angstrom-scale surface roughness and its increase may result in lowering of the reliability and reproducibility of self-assembly as a nanofabrication technique. Furthermore, a systematic investigation of the effect of surface roughness on self-assembly may be essential before it is employed as a reliable high density nanofabrication method. For example, in the case of BPM, ~20 nm features as obtained by self-assembly of PS-*b*-PDMS block copolymer will provide an areal density of ~400 Gb/in² on a surface with $R_{\text{rms}} < 5$ Å. To achieve areal densities of 1 Tb/in² and beyond in BPM, the bit size has to shrink to <12 nm. If self-assembly of block copolymers is employed to achieve such high areal densities and small bit sizes, we speculate that tighter control over the surface roughness of magnetic media will become necessary.

Methods

Magnetic media fabrication and characterization. CoCrPt-SiO₂ media samples were grown on 0.5 mm thick glass substrates in a BPS Circulus M12 magnetron sputtering system. Granular FePt-C-Cu and FePt-C media samples were grown in an AJA Orion sputtering system. The size of all the media samples was 1 cm × 1 cm. X-ray diffraction, magneto-optical Kerr effect and alternating gradient force magnetometer were used to characterize the deposited films for their orientation and measuring out-of-plane coercivity.

PS-*b*-PDMS block copolymer preparation and its solvent annealing. PS-*b*-PDMS of molecular weight 51.5 kg/mol with PDMS volume fraction of 16% was chosen for the study as it leads to spherical morphology of the PDMS block in PS matrix². The presence of silicon in PDMS provides a high etch selectivity between the blocks. Moreover, the Flory-Huggins factor for phase separation of the blocks is large (0.26) compared to other block copolymers.

A 2.1 wt% solution of PS-*b*-PDMS in toluene was spun on the magnetic media (with or without TranSpin) to give ~54 nm thick film. The block copolymer film was solvent annealed in tetrahydrofuran (THF) and 6 : 1 toluene-heptane solvent mixture for 9 hours. This was followed by a two-step etching process. A thin layer of PDMS surfaces above the PS matrix and needs to be removed to be able to observe the dots underneath. CF₄ plasma (3 sccm) at 50 W was used for 5 seconds to remove the top PDMS layer. This was followed by O₂ plasma (20 sccm) at 90 W for 20 seconds to remove the PS matrix and oxidize the PDMS dots to SiO₂.

Surface characterization of magnetic media. A JEOL JSM6700F field-emission scanning electron microscope (FE-SEM) was used to acquire high resolution images of as-prepared as well as self-assembled structures. For roughness measurements, a Digital Instruments Nanoscope® IV atomic force microscope (AFM) was used in the tapping mode. Roughness data was extracted using Nanoscope Analysis software (supplied by Veeco Instruments). On each sample, a scan area of 2 μm × 2 μm was selected. To remove any tilt of the sample surface, a first-order plane fit was applied. For roughness analysis of an image, statistical values were calculated according to the heights of the pixel in the image. Two roughness parameters were studied - root mean

square roughness (R_{rms}) and peak-to-peak mean roughness depth (R_t). R_{rms} is the root mean square average of the height deviation from the mean image data plane. R_t is the average distance between the highest peak and lowest valley measured from the mean image data plane. The values of R_{rms} and R_t shown in Table 1 represent mean and standard deviation from eight scans at different locations on the sample.

- Ruiz, R. *et al.* Density multiplication and improved lithography by directed block copolymer assembly. *Science* **321**, 936–939 (2008).
- Bitá, I. *et al.* Graphoepitaxy of self-assembled block copolymers on two dimensional periodic patterned templates. *Science* **321**, 939–943 (2008).
- Segalman, R. A., Yokoyama, H. & Kramer, E. J. Graphoepitaxy of spherical domain block copolymer films. *Adv. Mater.* **13**, 1152–1155 (2001).
- Ross, C. A. *et al.* Si containing block copolymers for self-assembled nanolithography. *J. Vac. Sci. Technol. B* **26**, 2489–2494 (2008).
- Park, S. *et al.* Macroscopic 10-Terabit-per-square-inch arrays from block copolymers with lateral order. *Science* **323**, 1030–1033 (2009).
- Hirai, T. *et al.* One-step direct-patterning template utilizing self-assembly of POSS-containing block copolymers. *Adv. Mater.* **21**, 4334–4338 (2009).
- Jung, Y. S. & Ross, C. A. Well-ordered thin-film nanopore arrays formed using a block-copolymer template. *Small* **5**, 1654–1659 (2009).
- Wang, Q. *et al.* A simple pathway to ordered silica nanopattern from self-assembly of block copolymer containing organic silicon block. *Appl. Surf. Sci.* **256**, 5843–5848 (2010).
- Jung, Y. S. & Ross, C. A. Orientation-controlled self-assembled nanolithography using a polystyrene-polydimethylsiloxane block copolymer. *Nano Lett.* **7**, 2046–2050 (2007).
- Chuang, V. P., Gwyther, J., Mickiewicz, A. R., Manners, I. & Ross, C. A. Templated self-assembly of square symmetry arrays from an ABC triblock terpolymer. *Nano Lett.* **9**, 4364–4369 (2009).
- Chuanbing, T., Lennon, E. M., Fredrickson, G. H., Kramer, E. J. & Hawker, C. J. Evolution of block copolymer lithography to highly ordered square arrays. *Science* **322**, 429–432 (2008).
- Stipe, B. C. *et al.* Magnetic recording at 1.5 Pb m⁻² using an integrated plasmonic antenna. *Nature Photon.* **4**, 484–488 (2010).
- Hellwig, O. *et al.* Bit patterned media based on block copolymer directed assembly with narrow magnetic switching field distribution. *Appl. Phys. Lett.* **96**, 052511 (2010).
- Kamata, Y., Kikitsu, A., Hieda, H., Sakurai, M. & Naito, K. Ar ion milling process for fabricating CoCrPt patterned media using a self-assembled PS-PMMA diblock copolymer mask. *J. Appl. Phys.* **95**, 6705–6707 (2004).
- Stuen, K. O. *et al.* Graphoepitaxial assembly of asymmetric ternary blends of block copolymers and homopolymers. *Nanotechnology* **21**, 495301 (2010).
- Sundrani, D., Darling, S. B. & Sibener, S. J. Guiding polymers to perfection: macroscopic alignment of nanoscale domains. *Nano Lett.* **4**, 273–276 (2004).
- Hashimoto, T., Bodycomb, J., Funaki, Y. & Kimishima, K. The effect of temperature gradient on the microdomain orientation of diblock copolymers undergoing an order–disorder transition. *Macromolecules* **32**, 952–954 (1999).
- Mansky, P. *et al.* Large-area domain alignment in block copolymer thin films using electric fields. *Macromolecules* **31**, 4399–4401 (1998).
- Chen, Z. R., Kornfield, J. A., Smith, S. D., Grothaus, J. T. & Satowski, M. M. Pathways to macroscale order in nanostructured block copolymers. *Science* **277**, 1248–1253 (1997).
- Lin, Z. *et al.* A rapid route to arrays of nanostructures in thin films. *Adv. Mater.* **14**, 1373–1376 (2002).
- Kim, S. H., Misner, M. J. & Russell, T. P. Solvent-induced ordering in thin film diblock copolymer/homopolymer mixtures. *Adv. Mater.* **16**, 2119–2123 (2004).
- Peng, J., Han, Y., Knoll, W. & Kim, D. H. Development of nanodomain and fractal morphologies in solvent annealed block copolymer thin films. *Macromol. Rapid Commun.* **28**, 1422–1428 (2007).
- Bosworth, J. K. *et al.* Control of self-assembly of lithographically patternable block copolymer films. *ACS Nano* **2**, 1396–1402 (2008).
- Knoll, A., Magerle, R. & Krausch, G. Phase behavior in thin films of cylinder-forming ABA block copolymers: Experiments. *J. Chem. Phys.* **120**, 1105–1116 (2004).
- Jung, Y. S. & Ross, C. A. Solvent-vapor-induced tunability of self-assembled block copolymer patterns. *Adv. Mater.* **21**, 2540–2545 (2009).
- Hirayama, Y., Tamai, I., Takekuma, I. & Nakatani R. Role of underlayer for segregated structure formation of CoCrPt-SiO₂ granular thin film. *J. Phys.: Conf. Ser.* **165**, 012033 (2009).
- Fernandez, R., Amos, N., Zhang, C., Lee, B. & Khizroev, S. Optimization of L10-FePt/MgO/CrRu thin films for next-generation magnetic recording media. *Thin Solid Films* **519**, 8053–8057 (2011).
- Shi, J. Z., Piramanayagam, S. N., Mah, C. S. & Zhao, J. M. Influence of gas pressures on the magnetic properties and recording performance of CoCrPt-SiO₂ perpendicular media. *J. Magn. Magn. Mater.* **303**, e145–e151 (2006).
- Takahashi, Y. K., Ohnuma, M. & Hono, K. Ordering process of sputtered FePt films. *J. Appl. Phys.* **93**, 7580–7582 (2003).
- Yang, X., Xu, Y., Seiler, C., Wan, L. & Xiao, S. Toward 1 Tdot/in.² nanoimprint lithography for magnetic bit-patterned media: Opportunities and challenges. *J. Vac. Sci. Technol. B* **26**, 2604–2610 (2008).
- Park, S. M. *et al.* Sub-10 nm nanofabrication via nanoimprint directed self-assembly of block copolymers. *ACS Nano* **5**, 8523–8531 (2011).



32. Graubner, V.-M. *et al.* Wettability and surface composition of poly(dimethylsiloxane) irradiated at 172 nm. *Polym. Mater. Sci. Eng.* **88**, 488–489 (2003).
33. Farrell, R. A., Fitzgerald, T. G., Borah, D., Holmes, J. D. & Morris, M. A. Chemical interactions and their role in the microphase separation of block copolymer thin films. *Int. J. Mol. Sci.* **10**, 3671–3712 (2009).
34. Pease, R. F. & Chou, S. Y. Lithography and other patterning techniques for future electronics. *Proc. IEEE* **96**, 248–270 (2008).

Acknowledgements

This work has been funded by Singapore's National Research Foundation Grant no. NRF-CRP 4-2008-06. M.S.M.S. acknowledges further support by the IMRE-funded core project no. IMRE/09-1C0319. S.K. gratefully acknowledges the financial support of the NUS Research Scholarship for doing Ph.D. The authors wish to acknowledge the help of Dr. Ramesh Thamankar of Institute of Materials Research and Engineering, Singapore, for fruitful discussions on the physics of molecular motion.

Author contributions

R.G., H.H. and M.S.M.S. designed experiments. S.K. and N.G. performed experiments. S.K., R.G., M.S.M.S., H.Y. and C.S.B. analyzed the data. S.K. and M.S.M.S. wrote the main manuscript text and prepared figures. All authors reviewed the manuscript.

Additional information

Supplementary information accompanies this paper at <http://www.nature.com/scientificreports>

Competing financial interests: The authors declare no competing financial interests.

License: This work is licensed under a Creative Commons Attribution-NonCommercial-NoDerivative Works 3.0 Unported License. To view a copy of this license, visit <http://creativecommons.org/licenses/by-nc-nd/3.0/>

How to cite this article: Kundu, S. *et al.* Effect of angstrom-scale surface roughness on the self-assembly of polystyrene-polydimethylsiloxane block copolymer. *Sci. Rep.* **2**, 617; DOI:10.1038/srep00617 (2012).